

## PAPER

# On Optimal Magnitude of Fluctuations in Probe Packet Arrival Intervals\*

Kohei WATABE<sup>†a)</sup>, Student Member and Masaki AIDA<sup>††b)</sup>, Member

**SUMMARY** Active measurement is an end-to-end measurement technique that can estimate network performance. The active measurement techniques of PASTA-based probing and periodic-probing are widely used. However, for the active measurement of delay and loss, Baccelli et al. reported that there are many other probing policies that can achieve appropriate estimation if we can assume the non-intrusive context (the load of the probe packets is ignored in the non-intrusive context). While the best policy in terms of accuracy is periodic-probing with fixed interval, it suffers from the phase-lock phenomenon created by synchronization with network congestion. The important point in avoiding the phase-lock phenomenon is to shift the cycle of the probe packet injection by adding fluctuations. In this paper, we analyse the optimal magnitude of fluctuations corresponding to the given autocovariance function of the target process. Moreover, we introduce some evaluation examples to provide guidance on designing experiments to network researchers and practitioners. The examples yield insights on the relationships among measurement parameters, network parameters, and the optimal fluctuation magnitude.

**key words:** active measurement, fluctuation, probe packet, periodicity

## 1. Introduction

Packet loss rate and delay are important factors that decide service performance since high values can trigger the dropping of audio and video frames, particularly in real time communication services like video conferencing. Consequently, a detailed analysis of the loss and delay generated in actual networks has obvious benefits for the design of loss and delay sensitive applications, and it is useful also from the viewpoint of traffic management. However, it is inherently difficult to gather information related to loss and delay, because the Internet is composed of multiple networks that are managed by different Internet Service Providers (ISP) or other organizations. Therefore, we need a way that offers end-to-end measurements of the Quality of Service (QoS), which includes delay and loss.

Active measurement is an end-to-end measurement technique that can estimate the QoS of a network path. Active measurement derives the QoS from information ob-

tained by injecting probe packets into the target network path [1]–[5]. From the delay/loss experienced by probe packets, active measurement can estimate one-way delay, Round-Trip Time (RTT), and loss rate on the network path. It can also estimate link capacity [6], [7] and available bandwidth [8], [9] from changes in the delay or interval of the probe packets.

Active measurement is easy for the end user to perform but it is not trouble free due to the tradeoff between accuracy and the number of probe packets. The load of the probe packets affects the path's performance. We cannot estimate the true performance since that state occurs only without the probe stream. If we inject a lot of probe packets to increase the probing rate, the estimation accuracy would suffer since the extra traffic becomes appreciable. We do not deal here with the overheads imposed by the probe stream, but we state that a high probing rate does not necessarily provide accurate measurement. A detailed discussion of overheads is given in reference [10]. Moreover, active measurements have great difficulty in determining the average loss rate because packet loss is a rare event and the rate is low in most current networks, especially in the Internet core. Long delay events are as rare as packet loss, and require many probe packets for detection.

Therefore, it is important to be able to achieve highly accurate measurements with a limited number of probe packets. Then many prior works focus on the optimization of the operation to provide more accurate estimation [11]–[17].

Work by Baccelli et al. [11], [12] gave an important suggestion on the accuracy of active measurement in assessing delay and loss. Two methods are now popular for determining probe timing in active measurement: PASTA-based probing and periodic-probing. PASTA-based probing is the probing policy that follows the well-known PASTA (Poisson Arrivals See Time Averages) property [18], i.e. the packet injection is a Poisson process (arrival intervals follow an exponential distribution), and periodic-probing is based on fixed probe packet intervals. A comparison of PASTA-based probing and periodic-probing was discussed in RFC [19] and prior work [20]. The works showed that periodic-probing might achieve more accurate measurement compared with PASTA-based probing though it can become synchronized with the target. The above discussions consider, however, only two alternatives. In recent work [11], Baccelli et al. indicated that there might be many other probing policies that can estimate true performance values given the

Manuscript received February 13, 2013.

Manuscript revised July 7, 2013.

<sup>†</sup>The author is with the Graduate School of Information Science and Technology, Osaka University, Suita-shi, 565-0871 Japan.

<sup>††</sup>The author is with the Graduate School of System Design, Tokyo Metropolitan University, Hino-shi, 191-0065 Japan.

\*The earlier version of this paper was presented at the 30th IEEE international Conference on Computer Communication (IN-FOCOM 2011) Mini-Conference.

a) E-mail: k-watabe@ist.osaka-u.ac.jp

b) E-mail: maida@sd.tmu.ac.jp

DOI: 10.1587/transcom.E96.B.3028

assumption of a non-intrusive context (the extra traffic of probe packets can be ignored). Moreover, according to the result in reference [12], the best policy in terms of accuracy is periodic-probing under the general condition. However, it may not be best overall because of the synchronization problem (the problem is referred to as the phase-lock phenomenon). To solve this problem, Baccelli et al. [12] proposed a probing policy that makes the probe packet intervals follow a parameterized Gamma distribution.

That is, Baccelli et al. provided multiple selections other than traditional PASTA-based probing and periodic-probing, and they suggested that the optimal probing policy might be one of the selections. The work has a serious problem with regard to practical measurements even though it represents a great advance in network measurement. Its weakness was that it failed to specify the optimal parameter of the Gamma distribution. Therefore, Gamma-probing has been unable to establish optimal probing policies.

In this paper, to provide guidance to researchers and practitioners regarding how they should inject probe packets, we analyse the fluctuation magnitude of optimal probing policy and clarify the relationships between the optimal fluctuation magnitude and the properties of the target process. The important point in avoiding synchronization is to shift probe packet periodicity by fluctuations. Baccelli et al. shift the periodicity by using a Gamma distribution to determine probe packet intervals. In our study, we introduce a probing policy that fluctuates the probe intervals by using a normal distribution and determine the optimal fluctuation magnitude for the target process. Our analysis is composed of the following three steps.

1. To define the optimal magnitude of fluctuations that are added to the timing of probe packets, we define an evaluation function that takes the phase-lock phenomenon into consideration.
2. We show our evaluation function is determined by the autocovariance function (ACF) of the target process and the probing policy. Moreover, we clarify the relationships between the optimal magnitude of fluctuations and ACF of target process.
3. We show some evaluation examples in which we change ACF, measurement period, and the number of probe packets variously. We provide some insights by clarifying the dependency of the optimal fluctuation magnitude on network/measurement parameters. These insights are useful for network researchers and practitioners in order to design experiments. Especially, for a situation where it is hard obtaining the knowledge of ACF on real measurement, we present the design criteria on the safe side in order to avoid the phase-lock phenomenon for various ACF.

We provide a detailed mathematical proof and simulation results on the validity of our method. We used some approximations to simplify the derivation of the optimal probing policy. Mathematical and simulation-based analyses show that the approximations are valid.

The rest of the paper is organized as follows. Section 2 introduces some prior works regarding probing strategies. Next, in Sect. 3, we verify the cause of the phase-lock phenomenon and describe a method to assess it. Section 4 explains probing policy with fluctuated probe intervals. Section 5 analyzes the relationships between fluctuation magnitude and the accuracy of active measurement, and provides a method to specify the optimal fluctuation magnitude. We confirm the validity of our approximations that we use to derive the optimal probing, through M/M/1 simulation, and show evaluation examples in Sect. 6. In Sect. 7, we discuss the generality of our results. We conclude the paper in Sect. 8.

## 2. Probing Policy and Accuracy of the Estimator

In this section, we overview the current state-of-the-art by introducing some prior works on probing strategies for active measurement.

PASTA-based probing and periodic-probing have been widely used as the probing policies for active measurement. These probing policies are described in RFCs [3], [19], respectively, and Roughan's work provided a comparison of the two policies [20] (periodic-probing is called uniform sampling in this). The key features of the PASTA-based probing and periodic-probing are as follows.

- **PASTA-based probing;** The probe packet intervals follow an exponential distribution, i.e. the probe packet arrivals process follows a Poisson arrival. It can provide bias-free measurement because of the PASTA property [18] but may be inferior in terms of estimation accuracy.
- **Periodic-probing;** This probing policy uses fixed probe packet intervals. It is easier to manipulate, and it may be superior to PASTA-based probing in terms of accuracy in many cases. However, it can suffer from the problem of synchronization with the target being measured.

It is unknown to this author how prevalent periodicities are in the modern Internet. However, some works reported theoretical grounds for their existence [21], [22]. Hence, there is the tradeoff between the two policies, and we cannot judge which probing policy is better.

Baccelli et al. investigated alternatives to the above two probing policies, and suggested that there are better policies than these two probing policies. They indicate that there are many distributions other than PASTA-based probing that can provide bias-free measurements if a non-intrusive context (the load of probe packets is insignificant) can be assumed [11]. This property is named Non-Intrusive Mixing Arrivals See Time Averages (NIMASTA). NIMASTA contains the following three assumptions.

1. The stochastic process that expresses the network state we are interested in (e.g. virtual delay and loss/no-loss indication) is stationary and ergodic. This process is

called the ground truth process.

2. The point process of probe packet arrivals  $\{T_i\}$  ( $i = 1, 2, \dots, m$ ) is stationary and *mixing*. Mixing is the requirement that guarantees joint ergodicity between the probe and ground truth processes (see reference [11] for details).
3. The last assumption is the non-intrusive context, i.e. we can ignore the impact of probe packet overhead. Namely, the ratio of the probe stream (extra traffic) to all streams is very small.

Under the above assumptions, it was proved that the following equation holds:

$$\lim_{m \rightarrow \infty} \frac{1}{m} \sum_{i=1}^m h(X(T_i)) = E[h(X(0))] \quad \text{a.s.}, \quad (1)$$

where  $X(t)$  and  $h$  are the ground truth process and an arbitrary positive function, respectively. If we can obtain  $X(T_i)$  (e.g. the delay of the probe packet or loss/no-loss of probe packet) from a probe packet injected at time  $T_i$ , (1) means that we can estimate  $E[h(X(0))]$  without bias by the injection of  $m$  probe packets. The only requirements placed on the point process of probe packet arrival  $\{T_i\}$  ( $i = 1, 2, \dots$ ) are that it be stationary and mixing. Therefore, there are many point processes that can achieve unbiased estimation of ensemble mean  $E[h(X(0))]$  besides PASTA-based probing, inter-probe time follows an exponential distribution. Such mixing point processes include those whose intervals follow a Gamma distribution and a uniform distribution. Note that periodic-probing with fixed interval is not a mixing process, and does not satisfy (1).

Recent work [12] investigated how to select the optimal probing process. We can select the optimal (in terms of accuracy) probing process under a specific assumption by using the inter-probe time given by the parameterized Gamma distribution.

If we estimate the mean of  $X(0)$  by using active measurement, the estimator  $\hat{P}$  is

$$\hat{P} = \frac{1}{m} \sum_{i=1}^m X(T_i).$$

Thus the variance of  $\hat{P}$  is

$$\begin{aligned} \text{Var}[\hat{P}] &= \frac{1}{m^2} \text{Var} \left[ \sum_{i=1}^m X(T_i) \right] \\ &= \frac{1}{m^2} \sum_{i=1}^m \sum_{j=1}^m \text{Cov}(X(T_i), X(T_j)) \\ &= \frac{1}{m^2} \sum_{i=1}^m \sum_{j=1}^m \int_{-\infty}^{\infty} r(\tau) f_{i-j}(\tau) d\tau, \end{aligned} \quad (2)$$

where  $f_{i-j}$  is the probability density function (pdf) of  $T_i - T_j$ ,  $r(\tau) = \text{Cov}(X(t), X(t + \tau))$  is the ACF of the ground truth process  $X(t)$  (we can express  $r(\tau)$  by  $\tau$  alone, because  $X(t)$  is stationary) and the last equality follows from the stationary

property of  $X(t)$  and the probe packet process.

It was proved that no other probing process with an average interval  $d$  has a variance that is lower than that of periodic-probing [12]. Convexity of  $r(\tau)$  in real network is evidenced by the network measurement [12] and if  $r(\tau)$  is convex on the interval  $[0, \infty)$  and the average of the inter-probe time is  $d$ , the following inequality can be proven by using Jensen's inequality [23].

$$\begin{aligned} \int_{-\infty}^{\infty} r(\tau) f_k(\tau) d\tau &\geq r \left( \int_{-\infty}^{\infty} t f_k(t) dt \right) \\ &= r(kd) \\ &= \int_{-\infty}^{\infty} r(\tau) \delta(\tau - kd) d\tau, \end{aligned} \quad (3)$$

where  $\delta(\cdot)$  denote Dirac  $\delta$  function,  $k$  is a integer, and the first equality follows from the average inter-probe time  $d$  of probing. Therefore,  $f_{i-j}(\tau) = \delta(\tau - (i - j)d)$  minimizes (2), and it corresponds to periodic-probing. Estimator variance is associated with accuracy, lower is better, so periodic-probing is the best probing process if we focus only on variance. On the other hand, periodic-probing does not satisfy the assumptions of (1) due to non-mixing, so periodic-probing is not necessarily the best. This is because the phase-lock phenomenon may occur and the estimator may converge on a false value when the cycle of the ground truth process is synchronized with that of the probing process. For instance, if we inject the probe packets at time  $\{0, d, 2d, \dots\}$  by periodic-probing with inter-probe time  $d$  to measure a process  $X(t) = \sin(2\pi(t - S)/d)$  where  $S$  denotes random variable that follows a uniform distribution  $U(0, d)$ , the observed values take the same value  $X(0) = X(d) = X(2d) = \dots$ , and the estimator  $\hat{P}$  does not converge on  $E[X(0)] = 0$ . Namely, periodic-probing can become biased. Therefore, we cannot conclude that periodic-probing is always the optimal probing process.

To tune the tradeoff between PASTA-based probing and periodic-probing (which has bias but superior variance), Baccelli et al. proposed a probing process whose inter-probe time follows a parameterized Gamma distribution [12]. The pdf that is used as the interval between probe packets is given by

$$g(x) = \frac{x^{\beta-1}}{\Gamma(\beta)} \left( \frac{\beta}{d} \right)^{\beta} e^{-x\beta/d} \quad (x > 0), \quad (4)$$

where  $g(x)$  is the Gamma distribution whose shape and scale parameters are  $\beta$  and  $d/\beta$ , respectively.  $d$  ( $> 0$ ) denotes the mean, and  $\beta$  ( $> 0$ ) is the parameter. When  $\beta = 1$ ,  $g(x)$  reduces to the exponential distribution with mean  $d$ . When  $\beta \rightarrow \infty$ , the probing process reduces to periodic-probing because  $g(x)$  converges on  $\delta(x - d)$ . If ACF of  $X(t)$  is convex, it has been proven that the variance of estimator  $\hat{P}$  sampled by intervals that follow (4) monotonically decreases as  $\beta$  increases. We can achieve small variance (it approaches the variance of periodic-probing) by setting  $\beta$  to a large value since (4) converges on periodic-probing towards the limit

$\beta \rightarrow \infty$ . The problem of bias due to the phase-lock phenomenon can be avoided if we tune  $\beta$  to a limited value (the probing process that has intervals set by (4) is mixing). We can resolve the tradeoff between PASTA-based probing and periodic-probing if we give  $\beta$  an appropriate value. This Gamma-probing provides multiple selections lying between traditional PASTA-based probing and periodic-probing through parameter  $\beta$ , and it is a great advance in network measurement techniques.

However, since Ref. [12] did not indicate how to decide upon the optimal  $\beta$ , it has remained a problem with no solution. To solve this problem, we introduce in this paper a method that can specify the optimal probing policy.

### 3. Evaluation of Phase-Lock Phenomenon

This study examines the phase-lock phenomenon in detail because our goal, specifying the optimal probing process, demands avoidance of this phenomenon. Reference [12] did not mention this cause of the phase-lock phenomenon in detail because it was not main topic. Accordingly, this section investigates the cause and effect of the phase-lock phenomenon and introduces an evaluation function that can assess this phenomenon appropriately.

The convex ACF  $r(\tau)$  of the ground truth process  $X(t)$  means  $X(t)$  has no special periodicity (see Fig. 1). The phase-lock phenomenon occurs when the cycle of the ground truth process synchronizes to that of the probing process. Hence, the phase-lock phenomenon will not occur if the ACF is strictly convex. (3) showed that variance is minimized with periodic probing, and it means that it will not realize large variance (inaccuracy) due to phase-lock phenomenon, under the strictly convex ACF. However, the experiments in Ref. [12] demonstrated that there are multiple instances in which the accuracy of the estimator of periodic-probing was worse than that of other probing processes (periodic-probing is not always inaccurate).

We consider that the phase-lock phenomenon is caused by *accidental periodicity* that is realized by using finite measurement periods. Even if the ground truth process has no special periodicity (in terms of long-time average), accidental periodicity is possible. Thus, there is a possibility that a specific frequency component will be present by chance if the measurement period is limited. Even if ACF in terms of ensemble mean (namely long-time average)

$$r(\tau) = E[X(t)X(t + \tau)] - \{E[X(t)]\}^2$$

is strictly convex, ACF in terms of a time average on finite period  $(0, l]$

$$R(\tau) = \frac{1}{l - \tau} \int_0^{l-\tau} X(t)X(t + \tau)dt - \frac{1}{(l - \tau)^2} \int_0^{l-\tau} X(t)dt \int_0^{l-\tau} X(t + \tau)dt \quad (5)$$

is not necessarily convex. Note that  $R(\tau)$  is a stochastic process that depends on  $X(t)$ . If we measure the  $X(t)$  on limited measurement period  $(0, l]$ , we should consider (5) that is generated by  $X(t)$  on  $(0, l]$ . In Fig. 2, we display the ACF of M/M/1 queue length. The arrival rate and the service rate are 0.75 and 1.0, respectively. The line of time average in Fig. 2 represents the time average on a finite period  $(0, 10000]$  for a single sample path generated by simulation. According to the figure, we can confirm that the ACF in terms of a time average is not a convex function though the ACF exhibits, in terms of ensemble mean, convexity. In a sample path we show in the figure, we can find accidental periodicity at  $\tau \approx 250$ , and the estimator is inaccurate due to the phase-lock phenomenon if we set a probe interval to 250.

Unpredictability is what distinguishes accidental periodicity from special periodicity in terms of long-time average. Special periodicity continues into the future constantly since it reflects the structure of the target, and hence we can predict the cycle using knowledge of the past ground truth process. On the other hand, we cannot predict accidental periodicity, no matter what knowledge of past ground truth process we may use. Because the unexpected behavior that is the difference between the behavior of the real sample path and the expected behavior (that is expressed by ACF) yields accidental periodicity. If we can obtain knowledge of past ground truth process before a measurement, we can avoid synchronization with special periodicity by changing the cycle of the probing process. However, accidental periodicity cannot be predicted and can be generated on any cycle, and hence we cannot avoid synchronization with accidental periodicity by changing the cycle of the probing process.

Therefore, accuracy will fall if a sample path of the ground truth process contains a lot of frequency components to which the probing process can become synchro-

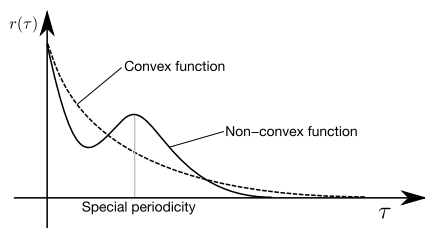


Fig. 1 Convexity of ACF and special periodicity of the ground truth process.

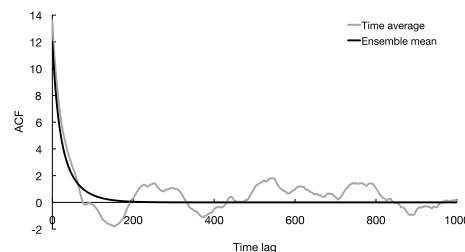


Fig. 2 ACF in terms of time average and ensemble mean.

nized. Conversely, if it contains few such frequency component, the accuracy will be remarkably high. The accuracy of periodic-probing may become extremely bad for the specific sample path though it is reasonable on average.

Accordingly, to assess the phase-lock phenomenon appropriately we must consider the accuracy that corresponding to the target sample path. We assume the metric that we want to measure is the time average  $\bar{X}_l = \int_0^l X(t)/l dt$  on the measurement period  $(0, l]$  and  $E[\hat{P}|X(t)] = \bar{X}_l$  holds (namely we can achieve bias-free measurement and the assumption suits our probing method which we will mention in Sect. 4). Note that our target  $\bar{X}_l$  is not ensemble mean  $E[X(0)]$  but empirical average, and it is random variables. By using a conditional variance, we can express the accuracy for the target sample path as

$$\text{Var}[\hat{P}|X(t)]. \quad (6)$$

Note that the conditional variance (6) is random variable that depends on stochastic process  $X(t)$ . We discriminate between accuracy regarding a time average and accuracy regarding an ensemble mean. The former is expressed by (6), and the latter is expressed by normal variance  $\text{Var}[\hat{P}]$ . Reference [12] proved that periodic-probing gives  $\text{Var}[\hat{P}]$  the minimal value (we introduced this in Sect. 2), and we can understand that  $\text{Var}[\hat{P}]$  corresponds to the expectation of the (6) according to the following equation:

$$E[\text{Var}[\hat{P}|X(t)]] = \text{Var}[\hat{P}] - \text{Var}[\bar{X}_l]. \quad (7)$$

Note that the second term on the right-hand side of (7) does not depend on the probing policy. Therefore, by using (7), we can assess the average accuracy (in which periodic-probing is superior). On the other hand, the effect of the phase-lock phenomenon is that (6) is varied with the intensity of the frequency component (which is synchronized with the probing process). The effect of the phase-lock phenomenon can be assessed by the following:

$$\text{Var}[\text{Var}[\hat{P}|X(t)]]. \quad (8)$$

This paper looks for a probing process that can avoid the extreme drops in accuracy created by the phase-lock phenomenon. In addition, the probing process should also achieve a small (7) (In other words, it should also be accurate in terms of average accuracy).

To find a probing policy that satisfies the above two requirements (which are assessed by (7) and (8), respectively), we introduce the following evaluation function:

$$\begin{aligned} & \{E[\text{Var}[\hat{P}|X(t)]]\}^2 + \text{Var}[\text{Var}[\hat{P}|X(t)]] \\ & = E\left[\{\text{Var}[\hat{P}|X(t)]\}^2\right]. \end{aligned} \quad (9)$$

Our evaluation function is defined by the square of  $l_2$ -norm of (8), and it is equivalent to Mean Square Error (MSE) with estimated parameter  $\theta = 0$ . We define the probing process that minimizes evaluation function (9) as the optimal probing process, and we investigate the optimal probing process

as determined by the property of the target network.

#### 4. Probing Method with Fluctuations

In this section, to analyse the optimal probing policy, we will introduce the probing process with fluctuated intervals that avoids the phase-lock phenomenon. As we mentioned in Sect. 3, the cause of the phase-lock phenomenon is accidental periodicity. We cannot avoid the phase-lock phenomenon by changing the cycle of the probing process (i.e. the average probe interval), since accidental periodicity can be generated on any cycle. Therefore, to avoid the phase-lock phenomenon, we use a random variable to fluctuate the probe intervals. In other words, we force the probing process to exhibit multiple cycles (i.e. variable intervals). Actually, the Gamma-probing proposed by Baccelli et al. in Ref. [12] is one approach to adding fluctuations. The method we introduce in this section takes three parameters into consideration: measurement period, number of probe packets, and fluctuation magnitude. It is expected that measurement period has a critical affect on the intensity of accidental periodicity. In terms of avoiding the phase-lock phenomenon, there is no essential difference between our approach and Gamma-probing, but our approach simplifies the analysis of the relationship between the evaluation function and the parameters of the probing policy.

We add fluctuations that obey a normal distribution to the timing of probe packet arrivals, while specifying the measurement period. We assume that the interval  $(0, l]$  is the measurement period and  $m$  is the number of probe packets sent in the measurement period. Our probing method gives the point process of probe packet arrivals  $\{T_i\}$  ( $i = 1, 2, \dots, m$ ) as follows.

$$T_i = S + G_i - l \left\lfloor \frac{S + G_i}{l} \right\rfloor, \quad (10)$$

where  $S$  and  $G_i$  denote the random variables that follow a uniform distribution  $U(0, l/m)$  and a normal distribution  $N((i-1)l/m, \sigma^2)$ , respectively,  $\lfloor \cdot \rfloor$  denotes a floor function and  $\sigma$  denotes the magnitude parameter of the fluctuations. To prevent  $\{T_i\}$  from taking a value outside the measurement period  $(0, l]$ , we add the third term. The second term contributes to the fluctuation of probe packet interval. The first term determines a phase, and does not affect the probe packet interval (note that the first term does not depend on  $i$ ). Note that the order of packet injection could be changed when the point process of probe packet arrivals is given by (10). The packets are injected in random order if the fluctuation magnitude is sufficiently large. It is easy to prove that the probability that at least one packet of  $m$  probe packets injects in  $[t, t + \Delta t)$  is  $(m\Delta t)/l$  for any  $t$  ( $0 \leq t < l$ ) since all of the phases are mixed uniformly by the random variable  $S$  if we inject the probe packets at  $\{T_i\}$  ( $i = 1, 2, \dots, m$ ) given by (10) (see Appendix). Therefore, estimator  $\hat{P} = \sum_{i=1}^m X(T_i)/m$  is an unbiased estimator for our target  $\bar{X}_l$ .

Our probing process provides multiple selections lying between traditional PASTA-based probing and periodic-probing as well as Gamma-probing. If  $\sigma = 0$  (namely there is no fluctuation),  $\{T_i\}$  corresponds to periodic-probing. On the other hand, if  $\sigma \rightarrow \infty$ ,  $T_i$  follows a uniform distribution  $U(0, l)$ . Therefore, intervals between  $T_i$  follow an exponential distribution for sufficiently large  $l$ .

**5. Fluctuation Magnitude and Accuracy**

In this section, we will clarify the relationship between fluctuation magnitude imposed on probe timing and the evaluation function (9), and we will detail a method that specifies the optimal fluctuation magnitude, theoretically. As we mentioned in Sect. 3, periodic-probing is the optimal probing process if we consider only average accuracy. It is important to specify the minimal fluctuation magnitude that can avoid the phase-lock phenomenon, because large fluctuations cause the probing process to deviate too far from periodic-probing.

Our evaluation function (9) is composed of the average and variance of (6). Therefore, we first address the stochastic behavior of (6). We define  $\tilde{X}_l(t) = X(t - l\lfloor t/l \rfloor)$  which depends on stochastic process  $X(t)$  in measurement period  $(0, l]$ . In addition, we define  $\tilde{T}_i = S + G_i$ , which is composed of a simple uniform and normal random variable. Since  $X(t)$  observed at the timing of  $\{T_i\}$  is equal to  $\tilde{X}_l(t)$  observed at the timing of  $\{\tilde{T}_i\}$ , the following equation holds:

$$\hat{P} = \frac{1}{m} \sum_{i=1}^m X(T_i) = \frac{1}{m} \sum_{i=1}^m \tilde{X}_l(\tilde{T}_i).$$

Therefore, by using ACF  $\tilde{R}_l(\tau) = \int_0^l \tilde{X}_l(t)\tilde{X}_l(t + \tau)/l dt - \{\int_0^l \tilde{X}_l(t)/l dt\}^2$  in terms of time average, (6) can be expressed as follows (as well as (2)).

$$\begin{aligned} \text{Var}[\hat{P}|X(t)] &= \frac{1}{m^2} \text{Var} \left[ \sum_{i=1}^m \tilde{X}_l(\tilde{T}_i) \middle| X(t) \right] \\ &= \frac{1}{m^2} \sum_{i=1}^m \sum_{j=1}^m \int_{-\infty}^{\infty} \tilde{R}_l(\tau) f_{i-j}(\tau) d\tau, \end{aligned}$$

where  $f_{i-j}$  is the pdf of  $T_i - T_j$ , and it obeys the normal distribution  $N((i - j)l/m, 2\sigma^2)$  when  $i \neq j$ . Note that  $\tilde{R}_l(\tau)$  is a stochastic process that depends on  $X(t)$ .

Furthermore, when we expand  $\tilde{R}_l(\tau)$  in Fourier series, we find that

$$\begin{aligned} \text{Var}[\hat{P}|X(t)] &= \frac{1}{m^2} \sum_{n=1}^{\infty} K_n \left\{ \sum_{i=1}^m \sum_{j=1}^m \int_{-\infty}^{\infty} \cos\left(\frac{2\pi n}{l}\tau\right) f_{i-j}(\tau) d\tau \right\}, \end{aligned} \tag{11}$$

$$K_n = \frac{2}{l} \int_0^l \cos\left(\frac{2\pi n}{l}\tau\right) \tilde{R}_l(\tau) d\tau,$$

where the second equality follows from the periodic and

even function  $\tilde{R}_l(\tau)$ . Note that  $\{K_n\} (n = 1, 2, \dots)$  are random variables that depend on  $X(t)$ ; they represent the intensity of each frequency component of  $X(t)$ . Since  $\tilde{T}_i - \tilde{T}_j = G_i - G_j (i \neq j)$  follows a normal distribution,  $N((i - j)l/m, 2\sigma^2)$ , the following equation holds:

$$\int_{-\infty}^{\infty} \cos\left(\frac{2\pi n}{l}\tau\right) f_k(\tau) d\tau = \int_{-\infty}^{\infty} \cos\left(\frac{2\pi n}{l}\tau\right) f_{m-k}(\tau) d\tau.$$

Therefore, we obtain

$$\begin{aligned} &\sum_{i=1}^m \sum_{j=1}^m \int_{-\infty}^{\infty} \cos\left(\frac{2\pi n}{l}\tau\right) f_{i-j}(\tau) d\tau \\ &= m \sum_{i=0}^{m-1} \int_{-\infty}^{\infty} \cos\left(\frac{2\pi n}{l}\tau\right) f_i(\tau) d\tau \\ &= m + m \int_{-\infty}^{\infty} \cos\left(\frac{2\pi n}{l}\tau\right) \sum_{i=1}^{m-1} \frac{1}{2\sigma\sqrt{\pi}} e^{-\frac{(\tau-il/m)^2}{4\sigma^2}} d\tau \\ &= m - m \int_{-\infty}^{\infty} \cos\left(\frac{2\pi n}{l}\tau\right) \frac{1}{2\sigma\sqrt{\pi}} e^{-\frac{\tau^2}{4\sigma^2}} d\tau \\ &\quad + m \int_{-\infty}^{\infty} \cos\left(\frac{2\pi n}{l}\tau\right) \sum_{i=0}^{m-1} \frac{1}{2\sigma\sqrt{\pi}} e^{-\frac{(\tau-il/m)^2}{4\sigma^2}} d\tau \\ &= \begin{cases} m + (m^2 - m) \int_0^{\infty} \cos\left(\frac{2\pi n}{l}\tau\right) \frac{1}{\sigma\sqrt{\pi}} e^{-\frac{\tau^2}{4\sigma^2}} d\tau, & n = mj \\ & (j = 1, 2, \dots) \\ m - m \int_0^{\infty} \cos\left(\frac{2\pi n}{l}\tau\right) \frac{1}{\sigma\sqrt{\pi}} e^{-\frac{\tau^2}{4\sigma^2}} d\tau, & \text{otherwise} \end{cases} \\ &= \begin{cases} m + (m^2 - m) e^{-\frac{(2\pi n)^2}{l^2} \sigma^2}, & n = mj \ (j = 1, 2, \dots) \\ m - m e^{-\frac{(2\pi n)^2}{l^2} \sigma^2}, & \text{otherwise} \end{cases}, \end{aligned} \tag{12}$$

where the last equality follows from the following integral (see Ref. [24]).

$$\int_0^{\infty} e^{-ax^2} \cos bx dx = \frac{1}{2} \sqrt{\frac{\pi}{a}} e^{-\frac{b^2}{4a}},$$

where  $a$  and  $b$  denote an arbitrary positive real number and an arbitrary real number, respectively.

Substituting (12) for (11), the accuracy achieved for target sample path  $\text{Var}[\hat{P}|X(t)]$  is expressed as follows using the intensity of each frequency component  $\{K_n\} (n = 1, 2, \dots)$ .

$$\text{Var}[\hat{P}|X(t)] = \sum_{i=1}^{\infty} w_i K_i, \tag{13}$$

$$w_i = \begin{cases} \frac{1+(m-1)e^{-\frac{(2\pi i)^2}{l^2} \sigma^2}}{m}, & i = mj \ (j = 1, 2, \dots) \\ \frac{1-e^{-\frac{(2\pi i)^2}{l^2} \sigma^2}}{m}, & \text{otherwise} \end{cases}.$$

Note that  $K_0 = 0$  because  $\int_0^l \tilde{R}_l(\tau) d\tau = 0$ .

To clarify the average and standard deviation of  $\text{Var}[\hat{P}|X(t)]$ , we must investigate the stochastic behavior of  $\{K_n\} (n = 1, 2, \dots)$ . Since Fourier transformation of autocorrelation function  $\tilde{R}_l(t) + \overline{X}_l^2$  of the stochastic process yields

a power spectrum (Wiener-Khintchin theorem [25]), the following equation holds for any sample path  $x(t)$  of  $X(t)$ ,

$$\mathcal{F} [\tilde{r}_l(t) + \bar{x}_l^2] = |\mathcal{F} [\tilde{x}_l(t)]|^2,$$

where  $\tilde{r}_l(t) + \bar{x}_l^2$  and  $\tilde{x}_l(t)$  represent the sample paths of  $\tilde{R}_l(t) + \bar{X}_l^2$  and  $\tilde{X}_l(t)$  that correspond to the sample path  $x(t)$ . Consequently,  $K_n$  relates to the Fourier coefficients of  $X(t)$  as follows.

$$K_n = \frac{C_n^2 + S_n^2}{2}, \tag{14}$$

where

$$C_n = \frac{2}{l} \int_0^l \cos\left(\frac{2\pi nt}{l}\right) X(t) dt,$$

$$S_n = \frac{2}{l} \int_0^l \sin\left(\frac{2\pi nt}{l}\right) X(t) dt.$$

Note that Fourier coefficients  $C_n$  and  $S_n$  are random variables because they depend on  $X(t)$ .

Hence, by using (13) and (14), we can express the evaluation function (9) by the covariance of  $C_i$  or  $S_i$ . (7) which composes our evaluation function is given as follows.

$$\begin{aligned} E[\text{Var}[\hat{P}|X(t)]] &= \sum_{i=1}^{\infty} w_i E\left[\frac{C_i^2 + S_i^2}{2}\right] \\ &= \frac{1}{2} \sum_{i=1}^{\infty} w_i \{ \text{Cov}(C_i, C_i) + \text{Cov}(S_i, S_i) \}. \end{aligned} \tag{15}$$

Similarly, the other component (8) forming the evaluation function is as follows.

$$\begin{aligned} \text{Var}[\text{Var}[\hat{P}|X(t)]] &= \sum_{i=1}^{\infty} \sum_{j=1}^{\infty} w_i w_j \text{Cov}\left(\frac{C_i^2 + S_i^2}{2}, \frac{C_j^2 + S_j^2}{2}\right) \\ &= \frac{1}{4} \sum_{i=1}^{\infty} \sum_{j=1}^{\infty} w_i w_j \{ \text{Cov}(C_i^2, C_j^2) \\ &\quad + 2 \text{Cov}(C_i^2, S_j^2) + \text{Cov}(S_i^2, S_j^2) \}. \end{aligned}$$

We assume that  $C_i$  and  $S_i$  follow normal distributions since it is difficult to treat covariance between the squares of random variables. We can provide the rationale of the approximation that  $C_i$  and  $S_i$  follow normal distributions. By separating the integrals, we get the following equations:

$$C_i = \frac{2}{l} \sum_{k=0}^{i-1} \int_{lk/i}^{l(k+1)/i} \cos\left(\frac{2\pi it}{l}\right) X(t) dt, \tag{16}$$

$$S_i = \frac{2}{l} \sum_{k=0}^{i-1} \int_{lk/i}^{l(k+1)/i} \sin\left(\frac{2\pi it}{l}\right) X(t) dt. \tag{17}$$

(16) and (17) are the summation of the  $i$  random variables

that obey the same distribution. Note that they are not independent of each other. Suppose that random variables  $X_k$  ( $k = 0, 1, \dots, n$ ) are stationary and  $\alpha$ -mixing with  $O(k^{-5})$ , and these expectation and the 12th moments are 0 and finite, respectively. The central limit theorem for dependent cases guarantees that the distribution of the summation  $X_{\text{sum}}^n = \sum_{k=1}^n X_k$  can approximate normal distribution for sufficiently large  $n$  [26]. The condition that is required for  $X_k$  is a sufficient condition, and the actual restriction is more relaxed (see Ref. [26] for details). The variance is given by

$$\text{Var}[X_{\text{sum}}^n] = n \left( E[X_1^2] + 2 \sum_{l=1}^{n-1} E[X_1 X_{1+l}] \right).$$

Therefore, if we assume

$$X_k = \int_{lk/i}^{l(k+1)/i} \cos\left(\frac{2\pi it}{l}\right) X(t) dt,$$

we can guarantee that the (16) follows a normal distribution for sufficiently large  $i$  (we can also guarantee the (17) follows a normal distribution similarly). Sufficient conditions for target process  $X(t)$  are as follows: (1) the target process  $X(t)$  is stationary process; (2) Variance of  $X(t)$  is finite; (3) the absolute value of ACF of  $X(t)$  is  $O(t^{-5})$ . Though we can not apply the above approximation for small  $i$ , we can consider that the (16) and (17) are summations of non-identically distributed  $h$  random variables with mean 0 by separating the integrals as follows.

$$C_i = \frac{2}{l} \sum_{k=0}^{h-1} \int_{lk/h}^{l(k+1)/h} \cos\left(\frac{2\pi it}{l}\right) X(t) dt,$$

$$S_i = \frac{2}{l} \sum_{k=0}^{h-1} \int_{lk/h}^{l(k+1)/h} \sin\left(\frac{2\pi it}{l}\right) X(t) dt.$$

The central limit theorem for non-identically distributed and independent random variables guarantees that the summation of random variables  $X_k$  follows a normal distribution when the following equation hold for some  $\delta > 0$  [26].

$$\lim_{n \rightarrow \infty} \frac{\sum_{k=0}^n E[|X_k - \mu_k|^{2+\delta}]}{\sqrt{\sum_{k=0}^n \nu_k^{2+\delta}}},$$

where  $\mu_k$  and  $\nu_k$  represent mean and variance of  $X_k$ . The above central limit theorems for dependent (but identically distributed) random variables and non-identically distributed (but independent) random variables motivate us to consider that (16) and (17) follow a normal distribution even though the explicit conditions to hold the central limit theorem for dependent and non-identically distributed random variables are not provided. Moreover, in Sect.6, we will supplement the rationale of the assumption through the simulation result.

By using the approximation, we can derive  $\text{Var}[\text{Var}[P|\hat{X}(t)]]$  as follows.

$$\text{Var}[\text{Var}[\hat{P}|X(t)]] = \frac{1}{4} \sum_{i=1}^{\infty} \sum_{j=1}^{\infty} w_i w_j \{ \text{Cov}(C_i^2, C_j^2)$$

$$\begin{aligned}
 &+ 2 \operatorname{Cov}(C_i^2, S_j^2) + \operatorname{Cov}(S_i^2, S_j^2) \} \\
 = &\frac{1}{4} \sum_{i=1}^{\infty} \sum_{j=1}^{\infty} w_i w_j \{ 2 \{ \operatorname{Cov}(C_i, C_j) \}^2 \\
 &+ 4 \{ \operatorname{Cov}(C_i, S_j) \}^2 + 2 \{ \operatorname{Cov}(S_i, S_j) \}^2 \},
 \end{aligned}$$

where the second equality follows from the property of the moment of bivariate normal distributions.

Finally, if we can relate  $\operatorname{Cov}(C_i, S_j)$ ,  $\operatorname{Cov}(C_i, C_j)$  and  $\operatorname{Cov}(S_i, S_j)$  to  $r(\tau)$ , our evaluation function can evaluate any probing method. Calculating  $\operatorname{Cov}(C_i, S_j)$ , we have

$$\begin{aligned}
 \operatorname{Cov}(C_i, S_j) &= \frac{4}{l^2} \int_0^l \int_0^l \cos\left(\frac{2\pi i}{l}t\right) \sin\left(\frac{2\pi j}{l}s\right) E[X(t)X(s)] \, ds dt \\
 &\quad - E[C_i]E[S_j] \\
 &= \frac{4}{l^2} \int_0^l \int_0^l \cos\left(\frac{2\pi i}{l}t\right) \sin\left(\frac{2\pi j}{l}s\right) r(s-t) \, ds dt \\
 &= \frac{4}{l^2} \int_0^l \int_{-t}^{l-t} \cos\left(\frac{2\pi i}{l}t\right) \sin\left(\frac{2\pi j}{l}(\tau-t)\right) r(\tau) \, d\tau dt \\
 &= \frac{2}{l^2} \int_0^l \int_{-l}^{-\tau} \left\{ \sin\left(\frac{2\pi(j+i)}{l}t + \frac{2\pi j}{l}\tau\right) \right. \\
 &\quad \left. + \sin\left(\frac{2\pi(j-i)}{l}t + \frac{2\pi j}{l}\tau\right) \right\} dt r(\tau) \, d\tau \\
 &\quad + \frac{2}{l^2} \int_{-l}^0 \int_{-\tau}^l \left\{ \sin\left(\frac{2\pi(j+i)}{l}t + \frac{2\pi j}{l}\tau\right) \right. \\
 &\quad \left. + \sin\left(\frac{2\pi(j-i)}{l}t + \frac{2\pi j}{l}\tau\right) \right\} dt r(\tau) \, d\tau.
 \end{aligned}$$

Moreover, by creating two cases  $i = j$  and  $i \neq j$  and integrating the result, we get  $\operatorname{Cov}(C_i, S_j) = 0$ . Similarly, we can calculate  $\operatorname{Cov}(C_i, C_j)$  and  $\operatorname{Cov}(S_i, S_j)$  as follows.

$$\begin{aligned}
 \operatorname{Cov}(C_i, C_j) &= \begin{cases} -\frac{2}{i\pi} r_{S,i} + \frac{4}{l} r_{C,i}, & (i = j) \\ \frac{4}{l\pi(j^2 - i^2)} (i r_{S,i} - j r_{S,j}), & (i \neq j) \end{cases}, \\
 \operatorname{Cov}(S_i, S_j) &= \begin{cases} \frac{2}{i\pi} r_{S,i} + \frac{4}{l} r_{C,i}, & (i = j) \\ \frac{4}{l\pi(j^2 - i^2)} (j r_{S,i} - i r_{S,j}), & (i \neq j) \end{cases}, \\
 r_{S,i} &= \int_0^l \sin\left(\frac{2\pi i}{l}\tau\right) r(\tau) \, d\tau, \\
 r_{C,i} &= \int_0^l \left(1 - \frac{\tau}{l}\right) \cos\left(\frac{2\pi i}{l}\tau\right) r(\tau) \, d\tau.
 \end{aligned}$$

Substituting them into (15), we have

$$\begin{aligned}
 E[\operatorname{Var}[\hat{P}|X(t)]] &= \sum_{i=1}^{\infty} \frac{4}{l} w_i r_{C,i}, \\
 \operatorname{Var}[\operatorname{Var}[\hat{P}|X(t)]] &= \sum_{i=1}^{\infty} \left\{ \frac{4}{l} w_i r_{C,i} \right\}^2 + \sum_{i=1}^{\infty} \left\{ \frac{2}{l\pi} w_i r_{S,i} \right\}^2 \\
 &\quad + \sum_{i \neq j} 16 w_i w_j \frac{(i^2 + j^2) \{ r_{S,i}^2 + r_{S,j}^2 \} - 4 i j r_{S,i} r_{S,j}}{l^2 \pi^2 (i^2 - j^2)^2}. \quad (19)
 \end{aligned}$$

However, the second and the third terms on the right-hand side of (18) are trivial compared with the first term if we give actual parameters to  $r(\tau)$ ,  $l$  and  $m$ . Hence, (18) is approximated as

$$\operatorname{Var}[\operatorname{Var}[\hat{P}|X(t)]] \approx \sum_{i=1}^{\infty} \left\{ \frac{4}{l} w_i r_{C,i} \right\}^2.$$

In Sect. 6, we will confirm the validity of the approximation.

Thus, the evaluation function  $e(\sigma)$  that corresponds to (9) is given by the following:

$$e(\sigma) = \left\{ \sum_{i=1}^{\infty} \frac{4}{l} w_i r_{C,i} \right\}^2 + \sum_{i=1}^{\infty} \left\{ \frac{4}{l} w_i r_{C,i} \right\}^2. \quad (20)$$

We can plot evaluation function  $e(\sigma)$  if we specify the following: measurement period  $l$ , number of probe packets  $m$ , the ACF  $r(\tau)$  of  $X(t)$ , and fluctuation magnitude  $\sigma$  (which is added to the timing of probe packets). This means that we can obtain the optimal fluctuation magnitude to suit the properties of the target network.

### 6. Approximation Validity and an Evaluation Examples

In this section, we confirm the validity of our approximations through simulation, and we will show an evaluation example. We should check the approximations that were used to derive (20). Moreover, at the end of this section, we show some examples of our evaluation function for the case of M/M/1 queue measurement.

We use the queue length (i.e. the number in the system) of M/M/1 as  $X(t)$ . The behavior of the M/M/1 queue is very well studied. The mean and variance of the queue length of an M/M/1 system are

$$\begin{aligned}
 E[X(t)] &= \frac{\rho}{1 - \rho}, \\
 \operatorname{Var}[X(t)] &= \frac{\rho}{(1 - \rho)^2}. \quad (21)
 \end{aligned}$$

The ACF of the queue length of an M/M/1 system is as follows [27].

$$r(\tau) = \frac{(\mu - \lambda)^3}{\pi} \int_0^{2\pi} \sin^2 \theta \frac{e^{-w|\tau|}}{w^3} \, d\theta,$$

where

$$w = \lambda + \mu - 2 \sqrt{\lambda \mu} \cos \theta.$$

Furthermore, if  $\mu = 1$ , we can approximate the normalized ACF by the following simple form (see (3.7) in Ref. [28]).

$$r'(\tau) \approx \frac{1}{2} \{ e^{-A|\tau|} + e^{-B|\tau|} \},$$

where

$$A = \frac{(1 - \lambda)^2}{1 + \lambda + \sqrt{\lambda}}, \quad B = \frac{(1 - \lambda)^2}{1 + \lambda - \sqrt{\lambda}}.$$



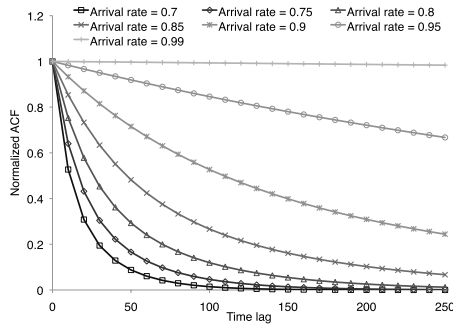


Fig. 3 Normalized ACFs of M/M/1 queue process for various arrival rates.

Therefore, by using (21), we can get the ACF of the M/M/1 queue as follows.

$$r(\tau) \approx \frac{\rho}{(1 - \rho)^2} r'(\tau). \tag{22}$$

We show the normalized ACF for various arrival rates  $\lambda$  in Fig. 3. Generally, the most important parameter that characterizes each ACF is the rate that  $r(t)$  approaches to 0.

On active measurement of delay, the probe packets obtain information of the waiting time, not the number in the system. Compared to the queue length case, the correlation structure of the waiting time on the M/M/1 system is extremely complicated, and does not provide any additional insight for our study. Thus we choose the queue length process as the target in our verification, though it does not correspond to actual measurements completely.

We discuss the validity of our approximations by using the ACFs that are obtained from a M/M/1 queue length. To derive (20), we used two approximations. One is a Fourier coefficient, which obeys a normal distribution, and the other is negligible terms on the right-hand side of (18).

First, we confirm that Fourier coefficients  $C_n$  and  $S_n$  obey normal distributions. We already showed the analytical rationale by using the extended central limit theorem in Sect. 5. We executed an M/M/1 simulation 3000 times and calculated the CDF of the  $C_1$  through the simulation. The CDF calculated through the simulation and the CDF of a normal distribution are displayed in Fig. 4. The parameters we used in the simulations are as follows. The arrival rate  $\lambda$  is 0.75, the service rate  $\mu$  is 1.0, and the simulation time is 50000. According to the figure, we confirm that these distributions are corresponding to each other. We gained similar results for  $C_n$  ( $n = 1, 2, \dots$ ). In Sect. 5, we used the property of moment of bivariate normal distributions with the approximation, i.e. we considered  $\text{Cov}(C_i^2, C_j^2) = 2\{\text{Cov}(C_i, C_j)\}^2$  and the other version of the combination of  $C_i$  and  $S_i$ . To verify the approximation accuracy, we executed an M/M/1 simulation 3000 times, and computed  $\text{Var}[C_n^2]$  and  $2\{\text{Var}[C_n]\}^2$  directly. Note that  $\text{Var}[C_n^2]$  and  $2\{\text{Var}[C_n]\}^2$  are special cases of  $\text{Cov}(C_i^2, C_j^2)$  and  $2\{\text{Cov}(C_i, C_j)\}^2$ , respectively. Figure 5 displays  $\text{Var}[C_n^2]$  and  $2\{\text{Var}[C_n]\}^2$  through the simulations. From Fig. 5, we can confirm that  $\text{Var}[C_n^2]$  is

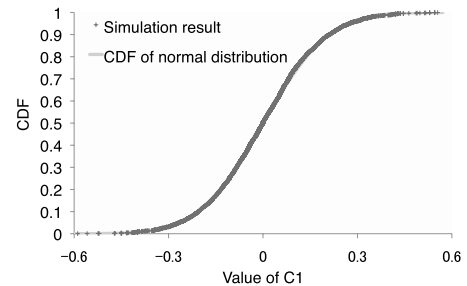


Fig. 4 CDF of the  $C_1$  calculated through the simulation.

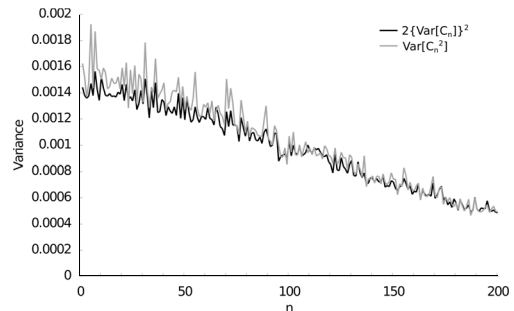


Fig. 5 Comparison of  $\text{Var}[C_n^2]$  and  $2\{\text{Var}[C_n]\}^2$ .

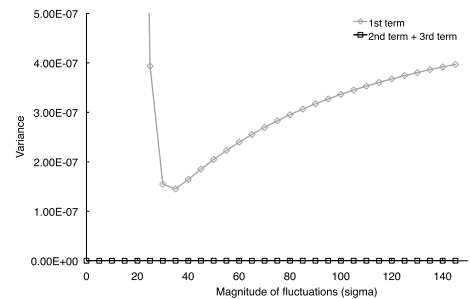


Fig. 6 Comparison of first term and other terms on the right-hand side of (18).

close to  $2\{\text{Var}[C_n]\}^2$ , for every  $n$ . We plotted  $\text{Var}[S_n^2]$  and  $2\{\text{Var}[S_n]\}^2$ , and gained similar results.

Furthermore, we show that the second and the third terms on the right-hand side of (18) are negligible. By using (22), we computed the first term and other terms on the right-hand side of (18) separately. Figure 6 represents the first term and other terms. The parameters we used are as follows. The arrival rate  $\lambda$  is 0.75, the service rate  $\mu$  is 1.0, the measurement period  $l$  is 50000, and the probing rate  $m/l$  is 0.01. Note that the horizontal axis represents the fluctuation magnitude  $\sigma$ . According to the figure, it is clear that the effects of the second and the third term are much less than those of the first term.

Next, we show the complementary cumulative distribution function (CDF) of the accuracy that is expressed by (6) in the case of the M/M/1 queue measurement in Fig. 7. The parameters we used are as follows. The arrival rate  $\lambda$  is 0.75, the service rate  $\mu$  is 1.0, the measurement period  $l$  is 1000, and the probing rate  $m/l$  is 0.01. We plotted for three differ-

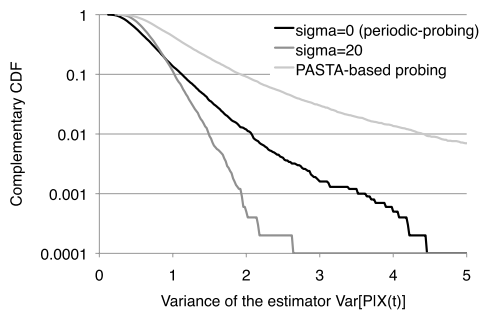


Fig. 7 Distribution of (6) in the case of the M/M/1 queue measurement.

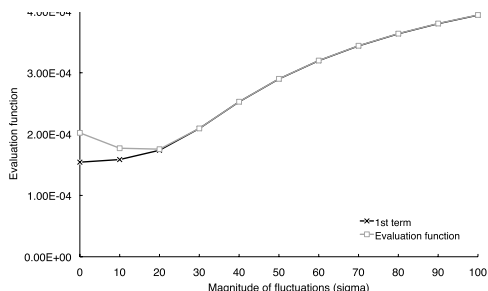


Fig. 8 Comparison of first term and other terms on the right-hand side of (20).

ent probing policies: periodic-probing, our probing method with  $\sigma = 20$  and PASTA-based probing. According to the figure, we can find that the variance  $\text{Var}[\hat{P}|X(t)]$  in the case of PASTA-based probing is so large (i.e. inaccurate), and larger variance in the case of periodic-probing occurs more frequently compared with that in the case of  $\sigma = 20$  (but the mean of the variance in the case of periodic-probing is smaller than that of  $\sigma = 20$ ). The result is consistent with our discussion in Sect. 3.

Finally, we show some examples of our evaluation function by using the ACFs that are obtained from a M/M/1 queue length. Please note that, in the rest of this section, we will not execute any simulation. We use the ACF that is derived from a M/M/1 queue process, but our result does not depend on any properties of M/M/1 except the ACF. Therefore, the result can be generalized to the processes that have similar ACF structure. These examples can provide us some insights for tuning the optimal fluctuation magnitude in actual measurements.

In Fig. 8, we display the evaluation function (20) with parameters of  $\lambda = 0.75$ ,  $\mu = 1.0$ ,  $l = 50000$ , and  $m = 500$ . We also plotted the first term of (20) (shown in the figure as crosses) in Fig. 8. Note that the horizontal axis represents the fluctuation magnitude  $\sigma$ . The first term of (20) expresses the square of the expectation of  $\text{Var}[P|X(t)]$  (it means the expectation of accuracy). According to Fig. 8, the first term is the smallest when  $\sigma = 0$  (i.e. the case of periodic-probing). On the other hand, our evaluation function is not the smallest because it assesses the phase-lock phenomenon by the second term. The evaluation function shows that the optimal value of  $\sigma$  is about 20 in this case.

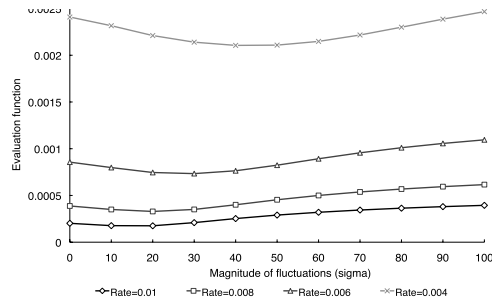


Fig. 9 Relationship between the optimal fluctuation magnitude and probing rate.

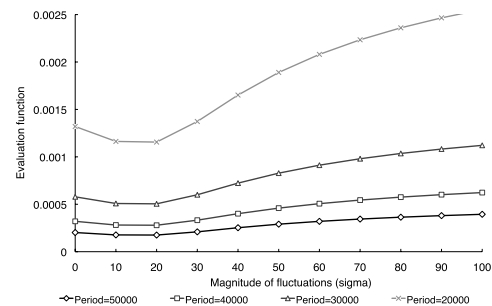
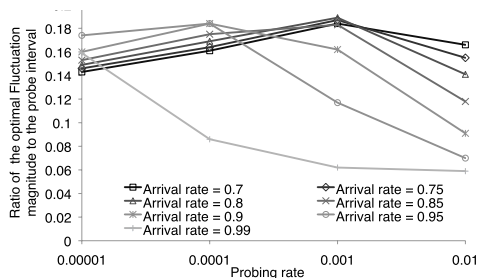


Fig. 10 Relationship between the optimal fluctuation magnitude and measurement period.

In addition, we verified the dependence of the evaluation function on each measurement parameter. First, we confirmed the relationship between the evaluation function and the probing rate  $m/l$ . We plot the evaluation function of each probing rate while changing  $m$  in Fig. 9. Parameters except  $m$  are as follows.  $\lambda = 0.75$ ,  $\mu = 1$ , and  $l = 50000$ . We can confirm that the optimal fluctuation magnitude decreases as the probing rate increases. Since the average probe packet intervals decrease with increase of the probing rate, the timing of probe packet injection is randomized with slight fluctuations when a probing rate is high. Adding fluctuations with magnitude  $\sigma$  to the probe packets with a rate  $m/l$  has a randomized effect equivalent to adding fluctuations with magnitude  $\sigma/2$  to the probe packets with a rate  $(2m)/l$ . Therefore, we can avoid the phase-lock phenomenon by adding slight fluctuations when a probing rate is high. Second, we confirmed the relation between the evaluation function and measurement period  $l$  with fixed probing rate. Figure 10 plots the evaluation function of each measurement period. Parameters except  $l$  are as follows.  $\lambda = 0.75$ ,  $\mu = 1$ , and the probing rate is 0.01. We can confirm that the optimal fluctuation magnitude holds steady even as the measurement period changes (if probing rate is fixed).

We show the dependence of the optimal fluctuation magnitude on traffic intensity to help network researchers and practitioners in designing experiments. As we mentioned above, the measurement period has no critical effect on the optimal fluctuation magnitude. Therefore, we can cover all cases if we consider the arrival rate and the



**Fig. 11** Ratio of the optimal fluctuation magnitude to the average probe intervals is less than 20%.

probing rate. In Fig. 11, we display the ratio of the optimal fluctuation magnitude to the average probe intervals  $l/m$  for each arrival rate. Namely, we plot  $m\sigma^*/l$  where  $\sigma^*$  is the optimal fluctuation magnitude. Note that the probing rate means the ratio of probe packet traffic to the regular traffic, since the service rate is fixed at 1 in our example. We plotted a wide variety of values of arrival rate in terms of the speed that ACF  $r(\tau)$  approaches to 0 (in Fig. 3, we showed the ACFs that correspond to the values of arrival rate we displayed). According to the Fig. 11, we can find that all of points are less than 20% though ACFs  $r(\tau)$  are extremely various. Practically, it is difficult to gain the exact knowledge of the ACF without a measurement. However, our result suggests that fluctuation magnitude corresponding to 20% is enough to avoid phase-lock phenomenon for a wide variety of ACFs.

We should take into account intrusiveness when we choose the probing rate  $m/l$ . High probing rate leads an accurate estimation normally though excessive injections of probe packets lead a deterioration of accuracy. In this paper, we present a method to specify the optimal fluctuation magnitude of probe packet intervals under the non-intrusive context (the load of the probe packets is ignored in the non-intrusive context). In real measurement, we must design experiments in which impact of the probe packet load is insignificant. Reference [10] clarified the relationship between an asymptotic variance and ACF of target process, and discussed the optimal probing rate that keeps the accuracy deterioration insignificant. According to the results in Ref. [10], in M/M/1 model with the arrival rate  $\lambda$  and the service rate  $\mu$ , an asymptotic variance  $s^2(\lambda, \mu, p)$  is given by the following if we inject probe packet with probing rate  $p\lambda$ .

$$s^2(\lambda, \mu, p) \approx \frac{\rho^2}{(1-\rho)^2} + p \frac{4\rho^3}{(1-\rho)^4}, \quad (23)$$

where  $\rho = (1+p)\lambda/\mu$ . The optimal probing rate is  $p\lambda$  that minimizes (23).  $p$  means the ratio of the probe stream to all streams, and the  $p$  that gives optimal probing rate provides insight to choose probing rate  $m/l$ .

## 7. Generality of the Result

We discuss generality of the result of M/M/1 model presented in Sect. 6. In Sect. 6, we presented the evaluation

examples based on the ACF of M/M/1 queue length process, and obtained some insights regarding the relationship among ACF, measurement period, the number of probe packets, and the optimal fluctuation magnitude. It is not the contention of this paper that the M/M/1 model is a good model for the modern networks. Of course, M/M/1 model is fundamental but unreal model and the modern networks are not well-modeled as it. However, the optimal fluctuation magnitude that specified by our method does not depend on any properties of M/M/1 except the ACF. Therefore, we obtain same results if the shape of ACF of process that we want to measure is similar to that of M/M/1 queue length process even if M/M/1 does not exactly model the inside of the target network (e.g. behavior of packet, network topology, and queueing, etc.).

The ACFs of processes that we are targeting are monotonically decreasing and convex functions on the interval  $[0, \infty)$  though our method that presented in Sect. 5 can apply to a process with any ACF. Monotonically decreasing and convex ACFs of delay/loss processes are well-motivated by analysis of real Internet traffic [12]. The most important parameter to characterize these ACFs is decreasing rate for  $\tau \rightarrow \infty$ .

ACF (22) of M/M/1 queue length process is simple function that satisfies above two conditions, and it can have various decay rate by changing parameter  $\rho$  as shown in Fig. 3. We can consider that the family of ACFs (22) that are based on M/M/1 queue length process represents various ACFs that we are targeting since target ACFs are characterized by decay rate.

We can expect that the insights that we obtained in Sect. 6 can be utilized when we design experiments for measurements of delay/loss processes whose ACF is monotonically decreasing and convex. In Sect. 6, we gained two main insights: (1) the optimal fluctuation magnitude has robustness to a change of measurement period  $l$ ; (2) the fluctuation magnitude of 20% of the average probe interval is enough to avoid phase-lock phenomenon for various probing rate and ACFs that have a wide variety of decay rate. As we mentioned above, it is difficult to gain the exact knowledge of the ACF. However, these insights can apply to various target processes that have similar ACF structure even if we cannot gain the knowledge of the ACF. Therefore, we can design a measurement on the safe side by setting the fluctuation magnitude to 20% of probe intervals (needless to say, we can design experiments optimally if we can gain the knowledge of the ACF). In addition to above insights, we understand that the results of validation of approximation that the second and the third terms on the right-hand side of (18) are negligible can also apply to various target processes that have similar ACF structure.

## 8. Conclusion

In this paper, we analysed the optimal fluctuation magnitude that should be added to the timing of probe packets. For the analysis, we introduced a probing policy that randomly per-

turbs the timing of probe packets by using a normal distribution. Moreover, we defined an evaluation function that can well assess the phase-lock phenomenon, and we provided a method that can specify the optimal fluctuation magnitude by using the ACF of the target process that we want to measure.

We confirmed the validity of our method by applying it to M/M/1 queue measurement. Furthermore, we showed that the probing rate greatly affects the optimal fluctuation magnitude. The measurement period is not a critical parameter. Through our evaluation examples, we were able to find that a fluctuation magnitude of 20% of the average probe interval is enough to avoid the phase-lock phenomenon for a wide variety of ACFs.

In the future, we will validate the method in detail including verification on an actual network. To implement our probing policy as an actual measurement method, we need to know the ACF of the target process (delay or loss process etc.) because it is needed to specify the optimal probing policy. Thus we will determine how to estimate the properties of the target network from past measurement data.

## Acknowledgment

This work was supported by JSPS Grant-in-Aid for JSPS Fellows Grant Number 24 · 3184.

## References

- [1] G. Almes, S. Kalidindi, and M.J. Zekauskas, "A one-way delay metric for IPPM," RFC2679, 1999.
- [2] G. Almes, S. Kalidindi, and M.J. Zekauskas, "A one-way packet loss metric for IPPM," RFC2680, 1999.
- [3] V. Paxson, G. Almes, J. Mahdavi, and M. Mathis, "Framework for IP performance metrics," RFC2330, 1998.
- [4] J. Bolot, "Characterizing end-to-end packet delay and loss in the Internet," High Speed Networks, vol.2, no.3, pp.289–298, 1993.
- [5] V. Paxson, "End-to-end Internet packet dynamics," ACM SIGCOMM Computer Communication Review, vol.27, no.4, pp.139–152, 1997.
- [6] C. Dovrolis, P. Ramanathan, and D. Moore, "Packet-dispersion techniques and a capacity-estimation methodology," IEEE/ACM Trans. Netw., vol.12, no.6, pp.963–977, 2004.
- [7] R. Kapoor, L.J. Chen, A. Nandan, M. Gerla, and M.Y. Sanadidi, "CapProbe: A simple and accurate capacity estimation technique for wired and wireless environments," ACM SIGCOMM Computer Communication Review, vol.34, no.4, pp.67–78, 2004.
- [8] M. Jain and C. Dovrolis, "End-to-end available bandwidth: Measurement methodology, dynamics, and relation with TCP throughput," IEEE/ACM Trans. Netw., vol.11, no.4, pp.537–549, 2003.
- [9] V.J. Ribeiro, R.H. Riedi, R.G. Baraniuk, J. Navratil, and L. Cottrell, "pathChirp: Efficient available bandwidth estimation for network paths," Passive and Active Measurement Conference (PAM 2003) Workshop, San Diego, CA, USA, April 2003.
- [10] M. Roughan, "Fundamental bounds on the accuracy of network performance measurements," ACM SIGMETRICS Performance Evaluation Review, vol.33, no.1, pp.253–264, 2005.
- [11] F. Baccelli, S. Machiraju, D. Veitch, and J. Bolot, "The role of PASTA in network measurement," ACM SIGCOMM Computer Communication Review, vol.36, no.4, pp.231–242, 2006.
- [12] F. Baccelli, S. Machiraju, D. Veitch, and J. Bolot, "On optimal probing for delay and loss measurement," ACM Internet Measurement Conference (IMC 2007), pp.291–302, San Diego, CA, USA, Oct. 2007.
- [13] F. Baccelli, S. Machiraju, D. Veitch, and J. Bolot, "Probing for loss: The case against probe trains," IEEE Commun. Lett., vol.15, no.5, pp.590–592, 2011.
- [14] J. Sommers, P. Barford, N. Duffield, and A. Ron, "Improving accuracy in end-to-end packet loss measurement," ACM SIGCOMM Computer Communication Review, vol.35, no.4, p.157, Oct. 2005.
- [15] M. Hasib, J. Schormans, and T. Timotijevic, "Accuracy of packet loss monitoring over networked CPE," IET Commun., vol.1, no.3, pp.507–513, 2007.
- [16] J. Sommers, P. Barford, N. Duffield, and A. Ron, "A geometric approach to improving active packet loss measurement," IEEE/ACM Trans. Netw., vol.16, no.2, pp.307–320, April 2008.
- [17] B.M. Parker, S.G. Gilmour, and J. Schormans, "Measurement of packet loss probability by optimal design of packet probing experiments," IET Commun., vol.3, no.6, pp.979–991, 2009.
- [18] R.W. Wolff, "Poisson arrivals see time averages," Operations Research, vol.30, no.2, pp.223–231, 1982.
- [19] V. Raisanen, G. Grotefeld, and A. Morton, "Network performance measurement with periodic streams," RFC3432, 2002.
- [20] M. Roughan, "A comparison of poisson and uniform sampling for active measurements," IEEE J. Sel. Areas Commun., vol.24, no.12, pp.2299–2312, 2006.
- [21] S. Floyd and V. Jacobson, "Traffic phase effects in packet-switched gateways," ACM SIGCOMM Computer Communication Review, vol.21, no.2, pp.26–42, 1991.
- [22] S. Floyd and V. Jacobson, "The synchronization of periodic routing messages," IEEE/ACM Trans. Netw., vol.2, no.2, pp.122–136, 2002.
- [23] I.S. Gradshteyn, I.M. Ryzhik, A. Jeffrey, and D. Zwillinger, Table of Integrals, Series, and Products, Seventh ed., ch. 12, p.1066, Academic press, New York, USA, 1980.
- [24] I.S. Gradshteyn, I.M. Ryzhik, A. Jeffrey, and D. Zwillinger, Table of Integrals, Series, and Products, Seventh ed., ch. 3, p.488, Academic press, New York, USA, 1980.
- [25] H. Stark and F.B. Tuteur, Modern Electrical Communications: Theory and Systems, pp.421–422, Prentice Hall, 1979.
- [26] P. Billingsley, Probability and Measure, ch. 5, pp.366–382, Jhon Wiley & Sons, 1986.
- [27] P.M. Morse, "Stochastic properties of waiting lines," Operations Research Society of America, vol.3, no.3, pp.255–261, 1955.
- [28] J. Abate and W. Whitt, "The correlation functions of RBM and M/M/1," Stochastic Models, vol.4, no.2, pp.315–359, 1988.

## Appendix

We prove that the probability that at least one packet of  $m$  probe packets injects in  $[t, t + \Delta t)$  is  $(m\Delta t)/l$  for any  $t$  ( $0 \leq t < l$ ) when we inject the probe packets at  $\{T_i\}$  given by (10).

*Proof.* The probability that  $i$ th packet is injected in infinitesimal difference  $[t, t + \Delta t)$  ( $0 \leq t < l$ ) under the condition  $S = s$  is

$$\Delta t \cdot \sum_{k=-\infty}^{\infty} p_{\text{norm}} \left( t + kl - \frac{l(i-1)}{m} - s \right),$$

where  $p_{\text{norm}}(t)$  denotes a pdf of normal distribution with average 0 and standard deviation  $\sigma$ . Then, the probability that one of packet of  $m$  probe packets is injected in  $[t, t + \Delta t)$  under the condition  $S = s$  is

$$\Delta t \cdot \sum_{i=1}^m \sum_{k=-\infty}^{\infty} p_{\text{norm}} \left( t + kl - \frac{l(i-1)}{m} - s \right).$$

Therefore, since  $S$  follows a uniform distribution  $U(0, l/m)$ , the probability that one of packet is injected in  $[t, t + \Delta t)$  is as follow.

$$\begin{aligned} & \Delta t \cdot \frac{m}{l} \int_0^{\frac{l}{m}} \sum_{i=1}^m \sum_{k=-\infty}^{\infty} p_{\text{norm}} \left( t + kl - \frac{l(i-1)}{m} - s \right) ds \\ &= \Delta t \cdot \frac{m}{l} \int_0^l \sum_{k=-\infty}^{\infty} p_{\text{norm}} \left( t + kl - \frac{l(i-1)}{m} - s \right) ds \\ &= \Delta t \cdot \frac{m}{l}. \end{aligned}$$

□



**Kohei Watabe** received his B.E. and M.E. degrees in Engineering from Tokyo Metropolitan University, Tokyo, Japan, in 2009 and 2011. He has been a graduate student of the Graduate School of Information Science and Technology, Osaka University since April 2011. He has been a JSPS research fellow (DC2) since April 2012. He is a student member of the IEEE.



**Masaki Aida** received the B.S. degree in Physics and M.S. degree in Atomic Physics from St. Paul's University, Tokyo, Japan, in 1987 and 1989, respectively, and received the Ph.D. in Telecommunications Engineering from the University of Tokyo, Japan, in 1999. After joining NTT Laboratories in April 1989, he has been engaged in research on traffic issues in computer communication networks. From April 2005 to March 2007, he was an Associate Professor at the Faculty of System Design, Tokyo Metropolitan University. He has been a Professor of the Graduate School of System Design, Tokyo Metropolitan University since April 2007. He received the Best Tutorial Paper Award of IEICE Communications Society in 2013. Prof. Aida is a member of the IEEE, IEICE, and the Operations Research Society of Japan.